Phosphate removal from water by modified pine bark using ionic liquid analog

Antonis Karachalios[a,b], Mahmoud Wazne[c,*]

[a]W.M. Keck Geoenvironmental Laboratory, Center for Environmental Systems, Stevens Institute of Technology, Castle Point on Hudson, Hoboken, NJ 07030, USA
[b]Innovative Environmental Technologies Inc., 6151 Kellers Church Road, Pipersville, PA 19454, USA
[c]Department of Civil Engineering, School of Engineering, Lebanese American University, P.O. Box: 36, Byblos, Lebanon
Tel. +961 9 547 262 Ext. 2518; Fax: +961 9 546 262; email: mahmoud.wazne@lau.edu.lb

ABSTRACT

Pine bark (PB) wood residues were chemically modified and used as anion exchange resins to remove phosphate (PO_4^{3-}) from water. The modification process involved reacting a holine-based ionic liquid analog, comprised of a mixture of choline chloride derivative and urea, with natural PB in the presence of imidazole. Batch sorption tests showed that the modified PB has a maximum PO_4^{3-}–P uptake capacity of 2.09 mmol/g (64.8 mg g^{-1}). The changes at the surface of the PB due to chemical modification and phosphate uptake were monitored using Fourier transform infrared spectroscopy analysis and Zeta potential measurements. The adsorption was found to be concentration and ionic strength dependent, exothermic, spontaneous, and is best described by a pseudo-second-order kinetics. The modified residues were used for the removal of PO_4^{3-} from an effluent of a dairy farm anaerobic digester and from a wastewater treatment plant sludge centrate.

Keywords: Phosphate; Wastewater; Biosorbent; Adsorption; Pine bark

1. Introduction

Phosphorus discharge into various water streams contributes to nutrient pollution, which is one of the top three causes of water impairment in the USA [1]. Nutrient pollution results mainly from municipal and industrial water effluent discharge, agricultural activities, and rainfall run-off over urban and suburban areas where stormwater management is not required. Total phosphorus in the influent of wastewater treatment plants may vary over a wide range of concentration; however, for most domestic wastewaters it is typically around 10–15 mg L^{-1}. Cellular growth of activated sludge micro-organisms in the treatment process usually removes 1–2 mg L^{-1} of the influent phosphorus in domestic wastewaters, leaving more than 10 mg L^{-1} in the effluent [2]. Similarly, discharge from agricultural activities constitutes a major source of nutrient pollution. In fact, in 2008, US EPA reported that the majority of freshwater eutrophication is attributed to agricultural nutrients such as PO_4^{3-}. Nutrient pollution from agriculture results mainly from diffuse sources such as overuse of fertilizers and discharge from manure stockpiles at animal feeding operations. A common practice at animal feeding operations is the use of anaerobic digestion technology. During the anaerobic treatment

*Corresponding author.

process, organic nitrogen compounds are converted to ammonia, sulfur compounds are converted to hydrogen sulfide, and phosphorus to orthophosphates. The end products of anaerobic digestion are a methane rich gas for energy production, nutrient rich organic slurry, and other inorganic products [3]. However, because anaerobic digestion does not remove any nutrients during the waste transformation process, the digested effluent retains a high PO_4^{3-}–P concentration ranging from 20 to 300 mg L^{-1} [4]. Finally, rainfall could wash nutrients from residential lawns and impervious surfaces into nearby rivers and streams. The problem is aggravated during heavy rainfall events for cities with combined sewer overflow where excess wastewater, including raw sewage, is mixed with run-off and is discharged directly into nearby streams and rivers.

Various phosphorus removal technologies have been investigated for the reduction of phosphate discharge into the environment. These technologies include physical (filtration of phosphorus particulates and membrane technologies), chemical (precipitation and adsorption), and biological processes [5]. However, in recent years there has been an increasing interest in environment friendly methods to remove phosphate from water, such as low-cost by-products sorbents made from agricultural and wood residues. Agricultural and wood residues were also chemically modified to increase their phosphate uptake capacity [6,7].

The chemical modification of agricultural and wood residues often involves quaternization, which is accomplished by reacting the residues with a number of quaternary amine compounds. The amine compounds react with the –OH groups in the glucose moieties of cellulose in the residues. For example, Wartelle and Marshall [8] used CHMAC (N-3-chloro-2-hydroxypropyl-trimethylamonium chloride) as a quaternization agent to chemically modify a series of 12 agricultural by-products. Modified corn stover showed the highest PO_4^{3-}–P removal at 0.66 mmol/g. Yue et al. [9] treated giant reed with epichlorohydrin, N,N-dimethylformamide, ethylenediamine, and triethylamine to yield the resin. The modified giant reed showed a PO_4^{3-} removal capacity of 0.21 mmol/g. Wang et al. [10] reacted wheat residue with dimethylamine in N,N-dimethylformamide, using pyridine as a catalyst after cross-linking the wheat residue with epichlorohydrin. The developed biosorbent was found to be an effective anion exchange resin with an exchange capacity for NO_3^- of 2.08 mmol/g. Orlando et al. [11] followed a similar procedure and reported NO_3^- removal capacities of 1.41 and 1.32 mmol/g, for modified sugarcane bagasse and modified rice hulls, respectively. Baidas et al. [12] used modified giant reed prepared with epichlorohydrin, ethylenediamine,

and triethylamine to remove perchlorate (ClO_4^-) from water. The modified giant reed showed a ClO_4^- adsorption capacity of 1.70 mmol/g. However, all of the above techniques make use of hazardous solvents or reagents.

This research entails the use of chemically modified pine bark (MPB) for the removal of phosphate from water and the delineation of the phosphate removal process. The chemical modification was achieved by quaternization of pine bark (PB) wood residues using green chemistry [13]. The modification process involved, reacting an ionic liquid analog, based on a eutectic mixture of a choline chloride derivative and urea, with natural PB (*Pinus resinosa*) in the presence of imidazole catalyst. The use of choline chloride derivative and urea for the chemical modification process has the advantage of using nontoxic reagents in addition to using the solvent as both a reagent and solvent.

2. Materials and methods

2.1. Materials

All chemical reagents used were of ACS or better grade. Imidazole and 2-Chloroethyl trimethylamonium chloride reagents were obtained from Sigma–Aldrich; urea was obtained from Fisher Scientific. The PO_4^{3-}–P stock solution was prepared by dissolving the set amount of sodium phosphate monobasic (Na_2HPO_4) (Fisher Scientific) in deionized water. The raw PB was obtained from Drew's Violets, Comstock, MI, USA. The centrate of anaerobically digested sludge solids was obtained from Bergen county utilities authority, NJ, USA, whereas the effluent from a dairy farm anaerobic digester was obtained from EMG International, Inc., PA, USA. The centrate had PO_4^{3-}–P concentration and pH values of 22.7 mg L^{-1} and 7.48, respectively, whereas the dairy farm effluent had PO_4^{3-}–P concentration and pH values of 34.0 mg L^{-1} and 7.51, respectively.

2.2. Adsorbent preparation

The MPB was prepared from natural PB, which consisted of 29.9% cellulose, 40.5% lignin, and 18.1% hemicellulose. Cellulose was measured using the Anthrone Method [14], whereas hemicellulose was measured using the Preece method [15]. The lignin content was determined using the Klason Method [16]. The PB raw material was initially milled in a Wiley mill (Thomas Scientific, Swedesboro, NJ) and sieved to retain the 10–20 mesh fractions. The quaternization was conducted using an ionic liquid

analog, based on a eutectic mixture of a choline chloride derivative and urea. The deep eutectic solvent (DES) was prepared first by adding 12.96 g (0.08 mol) of Chlorocholine chloride (ClChCl) to 10.27 g (0.17 mol) of urea and the mixture was heated at a Thermolyne® Mirak™ hotplate, at 75°C and stirred occasionally for 30 min [13,17]. The ionic liquid analog was then allowed to cool to room temperature. The quaternization was commenced by adding 0.1 g of PB to 5 mL of DES followed by 0.392 g (5.7 mmol) of imidazole. The mixture was heated in a Fisher Scientific Hi-Temp Oil Bath at 150°C for 15 h and then cooled to room temperature. The quaternized lignocellulosic material was extracted from the eutectic solvent and washed with water.

2.3. Sorbent characterization

2.3.1. Fourier transform infrared spectroscopy

The infrared spectra of the unmodified pine bark (UPB), MPB, and phosphate-adsorbed MPB, in the solid phase, were collected using a ThermoNicolet Nexus 670 spectrometer equipped with a Centaurus microscope. The spectra were collected in transmission mode at a resolution of 4 cm^{-1} and 128 scans.

2.3.2. Zeta potential

The Zeta potential determinations were conducted using 1.25 g L^{-1} MPB and UPB suspensions in the presence and absence of 200 mg L^{-1} PO$_4^{3-}$–P solution. The suspensions were prepared and mixed in 30 mL bottles and placed on a rotator for 2 h at 25°C (preliminary experiments showed that the reaction reached equilibrium in less than 2 h). After mixing, the equilibrium pH of the samples was measured and aliquots of the equilibrated suspensions were passed through 11 μm filter paper (Whatman No. 1). The filter pore size was selected based on the Malvern Zetasizer particle size range limitation for Zeta potential measurement between 5 nm and 10 μm. One (1) mL of each filtrate was introduced into a polystyrene disposable cuvette (Sarstedt, Germany) and Zeta potential was measured by a Nano Zetasizer (Malvern, Worcestershire, UK) using dynamic light scattering (DLS). A monochromatic coherent He–Ne laser with a fixed wavelength of 633 nm was used as a light source. The intensity of scattered light was measured by a detector at 173°C and an auto-correlation function was accumulated for 10 s. All DLS measurements were conducted at 25°C. The Helmholtz–Smoluchowski relationship was applied to convert measured electrophoretic mobilities to Zeta-potential. All samples were prepared in duplicates.

2.4. Batch experiments

Preliminary batch test experiments were conducted to determine the optimum MPB dosage to be used in the sorption tests. Incremental amounts of MPB were added to different 50 mL plastic bottles containing 200 mg L^{-1} PO$_4^{3-}$–P solution. The ionic strength was adjusted to 0.01 mol using NaCl before the bottles were capped and placed on a planetary shaker table for a period of 24 h. After mixing, the suspensions were filtered using 0.45 μm nylon membrane filters and the PO$_4^{3-}$–P concentrations in the supernatant were measured using the Ascorbic Acid Method [18]. The optimum MPB dosage was determined at 1.25 g L^{-1}.

After determining the optimum MPB loading, kinetic batch experiments were carried out in 30 mL plastic bottles using PO$_4^{3-}$–P solutions of 100, 200, and 300 mg L^{-1} at the optimum sorbent dosages. The plastic bottles were mixed on a planetary shaker table mixer for 2 h, (preliminary experiments showed that the reaction was completed in less than 2 h), before the supernatant was analyzed for PO$_4^{3-}$–P. Similarly batch adsorption experiments were conducted to construct the PO$_4^{3-}$–P adsorption isotherms using the prepared sorbent. The optimum biosorbent dosage was used in addition to PO$_4^{3-}$–P solutions ranging from 20–480 mg L^{-1}. Finally, the effect of pH, temperature, and ionic strength were examined. Solution pH was adjusted using sodium hydroxide (NaOH) or hydrochloric acid (HCl).

The sorption amount q_t (mg g^{-1}) of adsorbed PO$_4^{3-}$ anions at any time is calculated according to Eq. (1):

$$q_t = \frac{(C_0 - C_e)}{m} \times V \tag{1}$$

The distribution coefficient K_d measures the sorbent's sorption capacity and is calculated from Eq. (2):

$$K_d = \frac{(C_0 - C_e)}{C_e} \times \frac{V}{m} \tag{2}$$

where C_0 is the initial concentration of PO$_4^{3-}$–P (mg L^{-1}). C_e is the equilibrium concentration of PO$_4^{3-}$–P (mg L^{-1}). V is the volume of the solution (L). m is the MPB dosage (g).

All samples were prepared in duplicates and average values were used in the modeling parts.

2.5. Desorption and reusability studies

For the desorption experiments, 20 mg of the spent sorbent was treated with 25 mL of various concentrations

of NaCl solution, allowed to equilibrate for 2 h, then filtrated and PO_4^{3-} content was determined. The spent sorbents for this study were prepared by equilibrating 0.125 g MPB with 100 mL PO_4^{3-}–P solution (200 mg L^{-1}) for 2 h. To determine the reusability of MPB, consecutive sorption–desorption cycles were conducted five (5) times with the same sorbent using fresh PO_4^{3-}–P solution (200 mg L^{-1}). Regeneration of the sorbent was carried out using 0.2 mol/L NaCl. All samples were prepared in duplicates.

3. Results and discussion

3.1. Adsorbent characterization

The FTIR spectra of the UPB and MPB are shown in Fig. 1(a). The UPB spectrum is characterized by a broad peak at 3,600–3,200 cm^{-1}, which is attributed to –OH stretching vibrations of polymeric compounds especially polysaccharides (cellulose) [19]. The band at 1,631 cm^{-1} is attributed to carbonyl stretching, while the band at 2,916 cm^{-1} is assigned to C–H stretching from CH$_2$ group, especially alkenes. The band at 1,422–1,416 cm^{-1} is of phenolic O–H and C–O stretching of carboxylates, while the peaks at 1,150–1,000 cm^{-1} are attributed to vibration of C–O–C and O–H of polysaccharides [20]. Upon modification, a significant reduction was observed in the intensity of the broad peak at 3,600–3,200 cm^{-1}, indicating functionalization of the methyl hydroxyl groups during the quaternization process with chlorocholine chloride. The reaction destroys a large number of –OH groups of the cellulose structure. Moreover, the peak at 1,468 cm^{-1} in MPB indicates the presence of aliphatic C-N vibration, the peak at 1,031 cm^{-1} is characteristic of the –CH$_2$–N$^+$H(CH$_3$)$_2$ functional group and a broad band of the skeletal vibration of quaternary ammonium salt can be observed at 1,060 cm^{-1} [21,22].

The FTIR spectrum of PO_4^{3-}-adsorbed MPB along with the MPB spectrum are shown in Fig. 1(b). For the first spectrum, there are two additional peaks that indicate the presence of the phosphate group on the surface of MPB. The first peak is present at 1,142 cm^{-1} and is attributed to P=O stretching, whereas the second peak at 925 cm^{-1} is attributed to P–OH stretching [21]. The presence of these peaks is a clear indication of the adsorption of PO_4^{3-} onto the MPB.

3.2. Zeta potential

The effect of PB modification with the quaternary amine functional group and the effects of pH on the surface charge were investigated using UPB and MPB suspensions in the presence and absence of 200 mg L^{-1}

PO_4^{3-}–P. The results of the Zeta potential measurements are shown in Fig. 2. The measured Zeta potential for the UPB registered negative values over the entire pH range (3–11). However, these values were significantly increased upon quaternization. The Zeta potential of UPB decreased from −16.8 to −40.0 mV as pH increased from 3.6 to 10.6, whereas the Zeta potential for the MPB decreased from +23.6 to −36.9 mV as pH increased from 3.9 to 10.7. Thus, the incorporation of the quaternary amine functional groups into the PB increased the surface charge. However, the Zeta potential values decreased when PO_4^{3-} was added to the MPB. The decrease in surface charge indicated neutralization of the positive functional groups by the adsorbed PO_4^{3-}. It appears that the phosphate species were more efficient at neutralizing the quaternary ammonium functional group positive charges than the Cl$^-$ ion during the Zeta potential measurements. Karthikeyan et al. [23] reported on the preferential sorption of phosphate species on cationized solid wood residues in the presence of other ions. They attributed the preferential sorption due to specific sorption mechanisms. Such specific sorption mechanism was not explored in this study.

3.3. Effect of sorbent dosage

Batch tests were conducted to determine the optimal MPB loading to be used in the study. The values of the partition coefficient K_d and the maximum uptake capacity q_e were calculated and plotted for various liquid-to-solid ratios (Fig. 3). Contrary trends were observed for the maximum uptake capacity and partition coefficient values. The partition coefficient K_d increased from approximately 310 mL/g at liquid-to-solid ratio of 0.5 g L^{-1} to approximately 380 mL/g at liquid-to-solid ratio of 5 g L^{-1}. Conversely, the maximum uptake capacity q_e decreased from approximately 55 mg g^{-1} at liquid-to-solid ratio of 0.5 g L^{-1} to approximately 25 mg g^{-1} at liquid-to-solid ratio of 5 g L^{-1}. The intersection of the two curves was found approximately at the liquid-to-solid ratio of 1.25 g L^{-1}. Therefore, 1.25 g L^{-1} was used in all batch tests. The UPB did not show any significant phosphate removal.

3.4. Adsorption kinetics

The sorption of PO_4^{3-} onto MPB was studied as a function of contact time for various PO_4^{3-}–P concentrations and the results are presented in Fig. 3. It appears that the sorption of PO_4^{3-} takes place in two distinct steps: a relatively fast one continuing up to approximately 20 min followed by a slower one that leads to the equilibrium state. The high initial uptake rate can be attributed to the higher active sites availability for
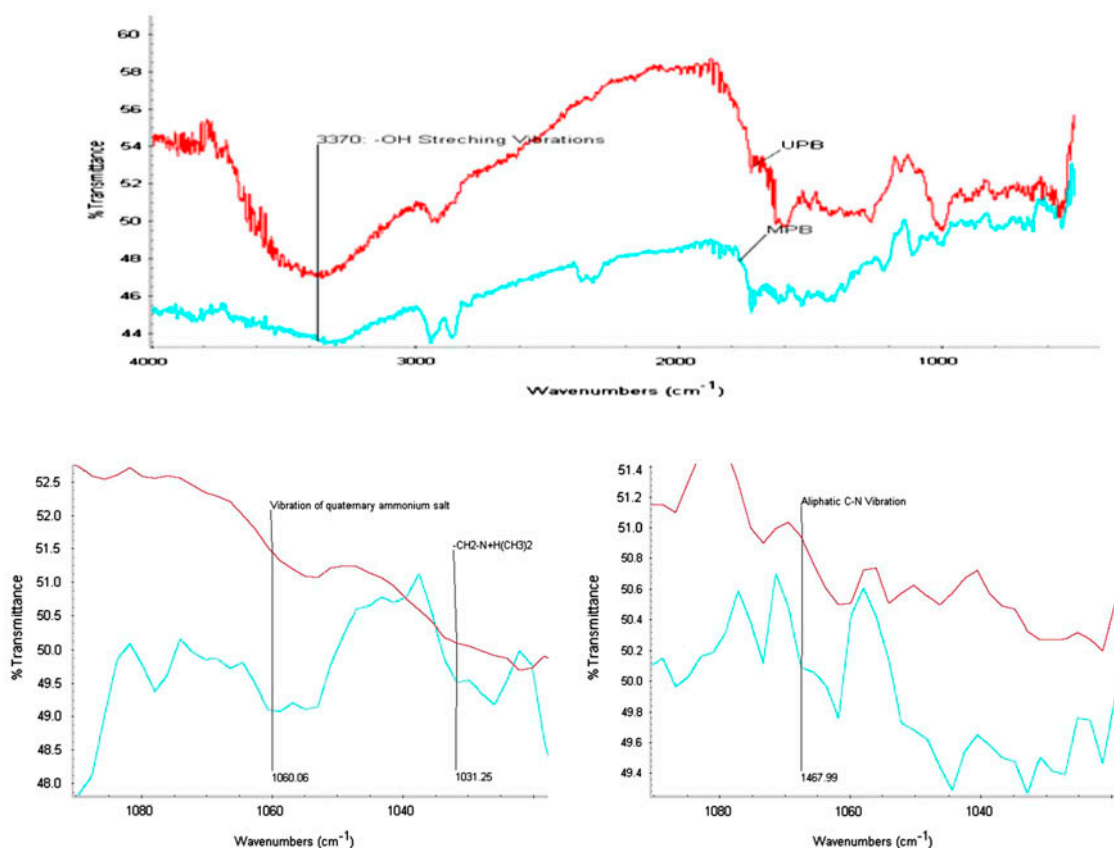
Fig. 1(a). FTIR spectra of UPB and MPB.

PO_4^{3-} sorption at the beginning of the process. The increase in PO_4^{3-}–P concentration resulted in an increase in the adsorption capacity. It appears that the increase in PO_4^{3-}–P concentration increases the diffusion of PO_4^{3-} from the bulk solution to the adsorbent due to the increase in the driving force of the concentration gradient [24].

Pseudo-first-order and second-order rate kinetic models were fitted to the 200 mg L^{-1} PO_4^{3-}–P uptake data. Fitting simple kinetic models such as first- or second-order rate equations to sorption on solid surfaces, which are rarely homogeneous, are often inappropriate because the effects of transport phenomena and chemical reactions are often experimentally inseparable [25]. Moreover, pseudo-kinetic models are also more appropriate when sorption is based on the solid sorbent capacity [26].

The experimental data was fitted by two kinetic models, a pseudo-first-order kinetic (Eq. (3)) and a pseudo-second order (Eq. (4)).

In the case of sorption preceded by diffusion through a boundary layer, the kinetics would most likely follow the pseudo-first-order equation of Lagergren [27]. The Eq. (3) for the pseudo-first-order kinetics model is presented below:

$$\ln(q_{e1} - q_t) = \ln q_{e1} - k_1 t \tag{3}$$

where q_t (mg g^{-1}) is the average uptake at time t, q_{e1} (mg g^{-1}) is the equilibrium uptake, k_1 (min^{-1}) is the reaction kinetic rate constant, and t (min) is the adsorption time. The above Lagergren rate equation is the most widely used rate equation for sorption of a solute from a liquid solution.

For a pseudo-second-order kinetics model based on solid sorption capacity, the rate expression can be expressed as Eq. (4) shows:

$$\frac{t}{q_t} = \frac{1}{k_2 q_{e2}^2} + \frac{t}{q_{e2}} \tag{4}$$

where k_2 (g mg^{-1} min^{-1}), is the pseudo-second-order rate constant. In Eq. (5), the expression $k_2 q_e^2$, the intercept term, describes the initial sorption rate, r (g mg^{-1} min^{-1}) as $t \rightarrow 0$.
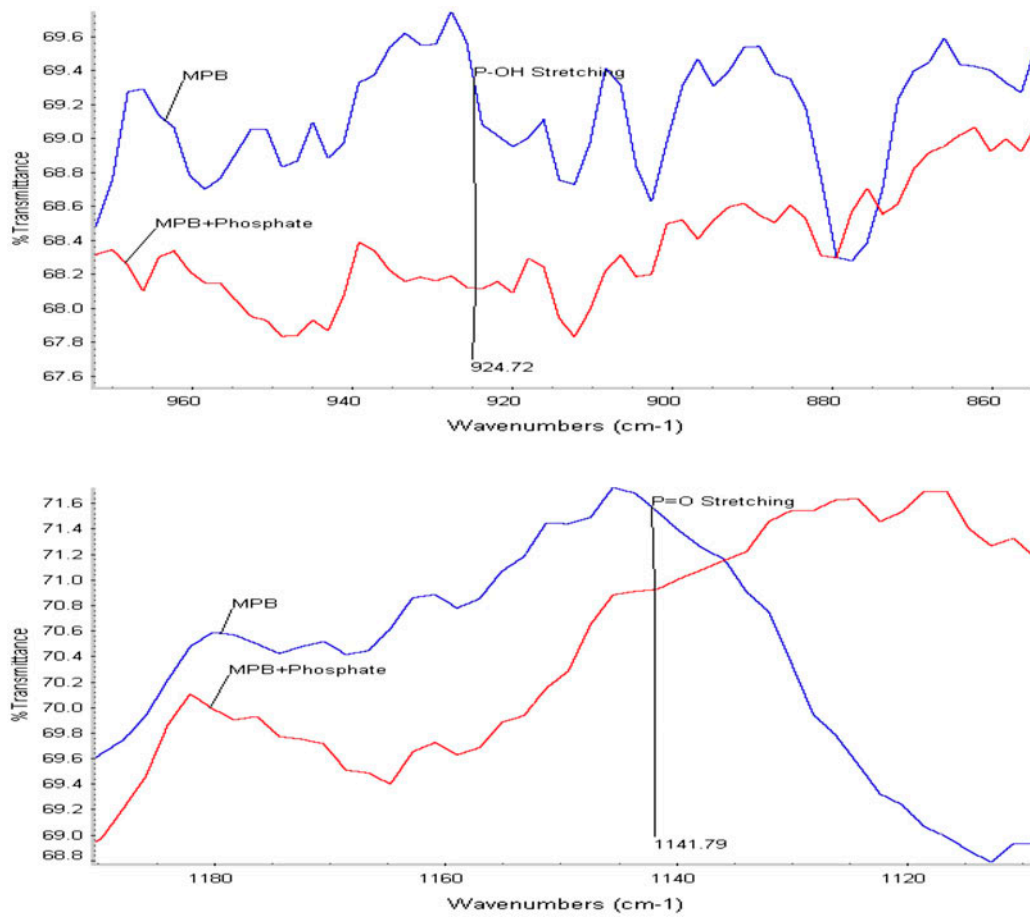
Fig. 1(b). FTIR spectra of MPB and phosphate-adsorbed MPB.
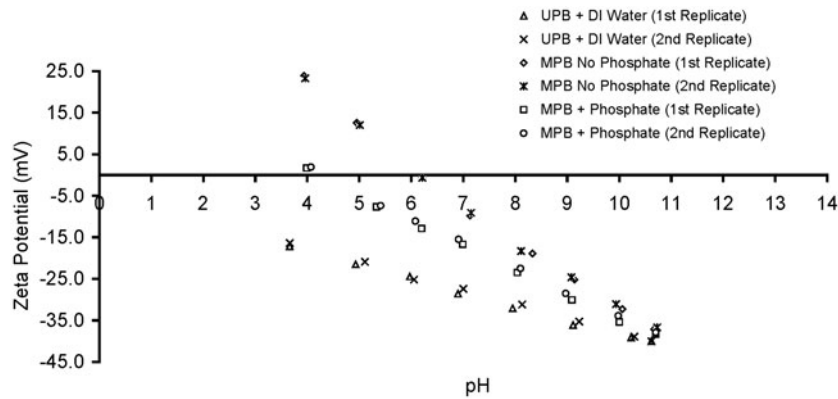
Fig. 2. Zeta potential for UPB and MPB.

$$r = k_2 q_{e2}^2 \tag{5}$$

The q_{e1} and k_1 values for the pseudo-first-order kinetic model were estimated by minimizing the sum of the squared residuals using the Microsoft Excel Solver tool. The estimated q_{e1} and k_1 values are shown in Table 1.

Even though the q_{e1} values were similar to the ones determined experimentally, the k_1 rates values did not appear to change with temperature. The k_1
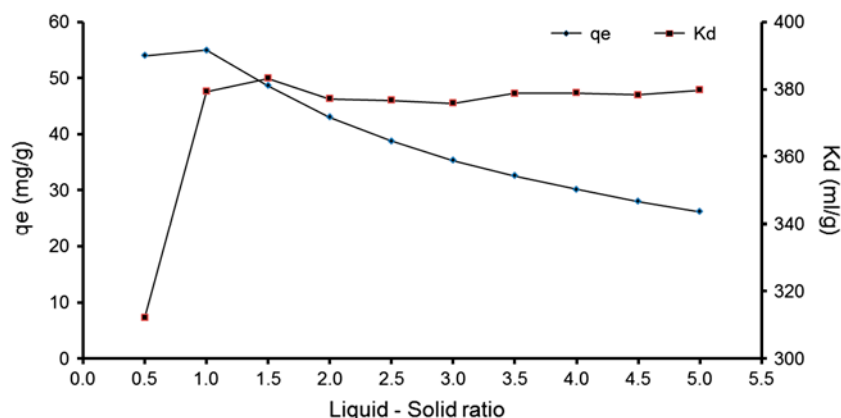
Fig. 3. Effect of sorbent dosage on PO_4^{3-}–P uptake by MPB.

values fitted by the model were estimated at 0.099, 0.098, and 0.120 for the reactions conducted at temperatures of 20, 40 and 60°C, respectively. Moreover, the (R^2) values calculated at 0.933, 0.739 and 0.759, respectively, did not indicate a good fit. For the pseudo-second-order kinetics model, the equilibrium sorption capacity (q_{e2}) and the rate constant (k_2) were calculated from the slope and intercept of the straight line described by Eq. (5). The calculated q_{e2} values were very close to the experimentally determined ones. The second-order model (R^2) values were calculated at 0.999, 0.999, and 0.999 for the reactions conducted at 20, 40 and 60°C, respectively. These values were much higher than the values determined for the first-order model, indicating a better fit. Moreover, the k_2 values showed an increasing trend with temperature, measured at 0.023, 0.031 and 0.037 for the reactions conducted at 20, 40 and 60°C, respectively. This indicates that the pseudo-second-order kinetic model is a better fit for the adsorption kinetics data [28].

Accordingly, the rate constants (k_2) of the pseudo-second-order model were used to calculate the activation energy (E_a) of the sorption process using the Arrhenius equation, which can be expressed from the following Eq. (6):

$$\ln k_2 = \ln A - \frac{E_a}{RT} \tag{6}$$

where A is the pre-exponential factor and R is the universal gas constant (8.314 J mol/K). E_a was calculated at 9.5 kJ/mol. This value fits well within the 8–16 kJ/mol energy range associated with ion-exchange sorption [29].

To further delineate the reaction mechanisms of PO_4^{3-} uptake by the biosorbent, an intraparticle diffusion model was fitted to the kinetic data [30] using Eq. (7):

$$q_t = k_{id} t^{0.5} \tag{7}$$

where k_{id} is the intraparticle diffusion rate constant (mg g^{-1}min$^{0.5}$).

The adsorption mechanism is generally considered to involve three steps where one or any combination of steps can be the rate-controlling mechanism: (i) mass transfer across the external liquid boundary layer; (ii) adsorption at a site on the surface; and (iii) diffusion of the adsorbate molecules on an adsorption site through the liquid-filled pores or the solid surface

Table 1
Kinetic parameters for PO_4^{3-}–P adsorption ($C = 200$ mg L^{-1})

PO_4^{3-}–P (200 mg L^{-1})°C	First-order equation			Pseudo-second-order equation			Intraparticle diffusion	Experiment data
	q_{e1} (mg g^{-1})	k_1 (min^{-1})	R^2	q_{e2} (mg g^{-1})	k_2 (g mg^{-1} min^{-1})	R^2	k_{id} (mg g^{-1} min^{-1})	q_e (mg g^{-1})
$T = 20$	56.3	0.099	0.933	56.8	0.023	0.999	16.95	56.2
$T = 40$	52.1	0.098	0.739	52.4	0.031	0.999	15.84	52.0
$T = 60$	50.1	0.120	0.759	50.5	0.037	0.999	15.63	50.1

[31]. If the rate-limiting step is intraparticle diffusion, a plot of the sorbed solute against the square root of the contact time should yield a straight line passing through the origin [28].

The plots of q_t against $t^{0.5}$ (Fig. 4) show that the relationship is not linear over the entire range of reaction time; consequently, intraparticle diffusion is not the rate-limiting step in the sorption process. The plot shows three straight parts indicating that three steps took place. The first, sharper portion was attributed to the diffusion of PO_4^{3-} through the solution to the external surface of adsorbent, i.e. the boundary layer diffusion of solute molecules. The second portion described the gradual adsorption stage, where intraparticle diffusion was rate limiting. The third portion was attributed to the final equilibrium stage for which the intraparticle diffusion started to slow down due to the extremely low PO_4^{3-} concentration left in the solution [21].

3.5. Effect of pH on phosphate removal

The effect of pH on PO_4^{3-}–P sorption capacity of MPB results are shown in Fig. 5. The maximum removal rate was obtained in the pH range 3.5–6.0. At higher pH values the PO_4^{3-}–P adsorption rates started decreasing. Different species of PO_4^{3-} exist in solutions including zero-valent H_3PO_4, monovalent $H_2PO_4^-$, divalent HPO_4^{2-}, and trivalent PO_4^{3-} phosphate species. At pH < 2 the dominant species in the system is H_3PO_4, which does not have high adsorption affinity to the active biosorbents sites. As pH increases, $H_2PO_4^-$ and HPO_4^{2-} become the predominant species, which have higher affinity for the active sites. In this pH range, phosphate removal becomes more favorable. When pH > 7 there appears to be an accelerated decrease of phosphate removal rates which can be attributed to the competition between the hydroxide groups and PO_4^{3-} anions for the active MPB sites [32] and the decrease of electrostatic attraction between the PO_4^{3-} anions and the MPB surface.
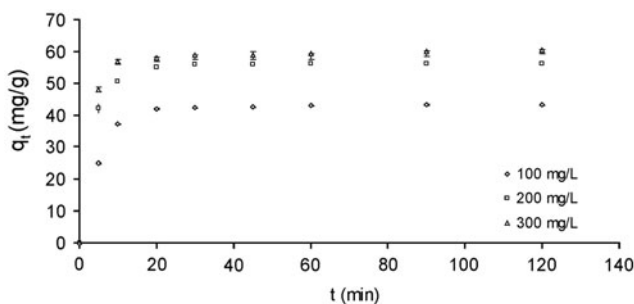
Fig. 4. Effect of contact time on PO_4^{3-}–P uptake by MPB.
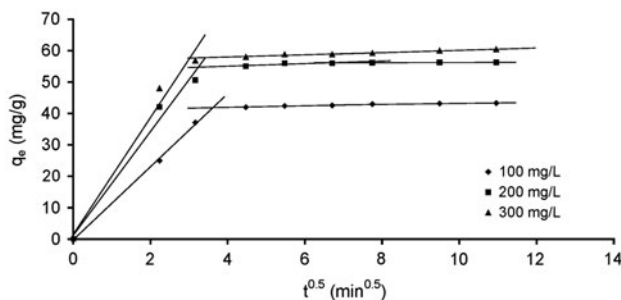
Fig. 5. Intraparticle diffusion model of PO_4^{3-}–P adsorption by MPB at $T = 20$ °C.

It is worth noting here that the modified residues may still contain pH-dependent groups such as hydroxyl, carboxyl, and phenolic functional groups, where these groups will exhibit greater negative charge as pH is increased resulting in reduced electrostatic attraction between the phosphate ions and the modified biosorbent. Similar results were reported by Xu et al. [33], Karthikeyan et al. [23] and Baidas et al. [12]. The modified PB showed similar nitrate uptake pH behavior by Karachalios et al. [13].

3.6. Adsorption isotherm

The adsorption isotherm experiments were conducted using PO_4^{3-}–P synthetic solutions at concentrations ranging between 0–480 mg L^{-1} and at three different temperatures (20, 40, and 60 °C). The results exhibited by the three curves (Fig. 6), displayed a continuous increase of PO_4^{3-}–P uptake until the three curves leveled off indicating site saturation. The highest uptake capacity was observed at $T = 20$ °C and was measured at 64.8 mg g^{-1} (2.09 mmol/g).

Langmuir and Freundlich adsorption models fit the adsorption data. The Langmuir model assumes monolayer adsorption on a surface containing a fixed number of binding sites. The maximum adsorption occurs upon monolayer saturation with no interaction occurring between the adsorbed sites. The linearized equation of the Langmuir sorption [34] model is expressed by the following Eq. (8):

$$\frac{C_e}{q_e} = \frac{1}{bq_m} + \frac{C_e}{q_m} \tag{8}$$

The Freundlich isotherm model [35] is an empirical relationship describing the sorption of solutes from a liquid to a solid surface and assumes that the adsorbent surface has multiple adsorption layers with the adsorption energy varying among the adsorption sites.
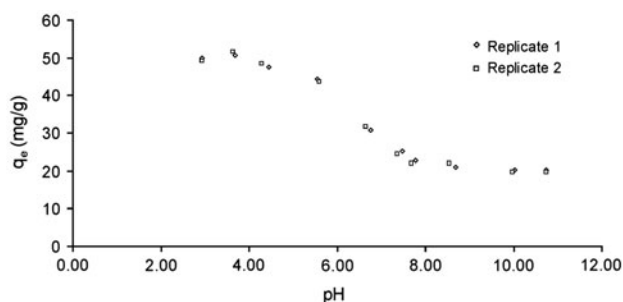
Fig. 6. Effect of pH on the PO_4^{3-}–P uptake by MPB.

The linear equation of the model is given by the following Eq. (9):

$$\ln q_e = \ln K_F - \frac{1}{n} \times t \ln C_e \qquad (9)$$

where q_e (mg g^{-1}) and C_e (mg L^{-1}) are the equilibrium concentrations of PO_4^{3-}–P in the solid and liquid phase, respectively, q_m (mg g^{-1}) is the measure of Langmuir monolayer sorption capacity, b (L^{-1} mg) is the equilibrium constant. K_F (mg g^{-1}(L^{-1} mg)$^{1/n}$) and n are characteristic constants related to the relative sorption capacity of the sorbent and the intensity of sorption, respectively. The correlation coefficients (R^2) and corresponding parameters are presented in Table 2.

The Langmuir model had higher correlation coefficients than the Freundlich model providing a better fit to the sorption data. These results indicated that the adsorption process occurring was likely monolayer adsorption on a surface with finite number of binding sites. Similar results were reported by Anirudhan et al. [21] for PO_4^{3-} adsorption on functionalized banana stems that underwent treatment with epichlorohydrin and dimethylamine followed by hydrochloric acid.

3.7. Effect of ionic strength on phosphate removal

The effect of the solution ionic strength on PO_4^{3-}–P removal was tested in batch experiments using 1.25 g L^{-1} loading of MPB and 200 mg L^{-1} PO_4^{3-}–P solution. The ionic strength was adjusted by changing the NaCl concentration. The results showed that the amount of PO_4^{3-} ions adsorbed decreased as the ionic strength increased. The PO_4^{3-}–P uptake decreased from approximately 63 mg g^{-1} to approximately 32 mg g^{-1}, as the ionic strength increased from 0 to 0.040 M (Fig. 7). Higher ionic strength creates a higher shielding effect for PO_4^{3-} ions adsorbing onto the MPB surface, which can cause a decrease in sorption; furthermore, the competition between increasing Cl$^-$ ions and PO_4^{3-} ions for the active sites on MPB might be responsible for the decrease [23] (Fig. 8).

3.8. Thermodynamic analysis

The PO_4^{3-} sorption onto the MPB was investigated at three different temperatures. The results showed decreasing trends in PO_4^{3-}–P sorption capacity with increasing temperature, which indicated that PO_4^{3-}–P sorption is more favorable at lower temperatures.

To evaluate the thermodynamic feasibility and understand the nature of the sorption process, three basic thermodynamic parameters, standard free energy ($\Delta G°$) (J/mol), standard enthalpy ($\Delta H°$) (J/mol), and standard entropy ($\Delta S°$) (J/mol K), were calculated using the following Eqs. (10, 11).

$$\Delta G° = \Delta H° - T\Delta S° \qquad (10)$$

$$\ln K_d = \left(\frac{\Delta S°}{R}\right) - \left(\frac{\Delta H°}{RT}\right) \qquad (11)$$

The values of $\Delta H°$ and $\Delta S°$ were determined from plots of $\ln K_d$ vs. $1/T$ along with the values of $\Delta G°$ (Table 3) and were derived from the Van't Hoff Equation [36].

The negative values of $\Delta H°$ indicate that the sorption process is exothermic and the spontaneous nature of the sorption process is evidenced by the negative values of $\Delta G°$. In addition, the positive values of $\Delta S°$ suggested an increase in the degree of freedom at the solid–liquid interface most likely resulting from the release of three chloride anions for the sorption of each PO_4^{3-} anion.

3.9. Desorption and reusability studies

Desorption tests were conducted using NaCl solutions with concentrations ranging between 0.1 and 2 mol/L [37]. The results indicated that 0.2 M NaCl solution effectively desorbed PO_4^{3-}–P from MPB at 99.8%. Reusability experiments were therefore conducted using 0.2 mol/L NaCl. After five consecutive sorption/desorption cycles, the sorption capacity decreased from 64.4 mg g^{-1} in the first cycle to 60.8 mg g^{-1} in the fifth cycle, while the recovery of the PO_4^{3-} ions decreased from 98.6 to 93.5%. No loss of MPB occurred during the five sorption/desorption cycles. The small amount of PO_4^{3-} not recovered during the regeneration experiments might have been caused by strongly bound PO_4^{3-}, resulting in a lower sorption capacity.

Table 2
Isotherm parameters for Langmuir and Freundlich equations

PO_4^{3-}–P (200 mg L^{-1}) (°C)	Freundlich equation ($q = KC^{1/n}$)			Langmuir equation ($q = q_m bC/(1 + bC)$)		
	K_F (mg g^{-1}(L^{-1} mg)$^{1/n}$)	n	R^2	q_m (mg g^{-1})	b (L^{-1} mg)	R^2
$T = 20$	2.92	3.22	0.925	67.1	0.058	0.999
$T = 40$	2.89	3.42	0.911	60.2	0.060	0.999
$T = 60$	2.84	3.66	0.947	55.9	0.042	0.993
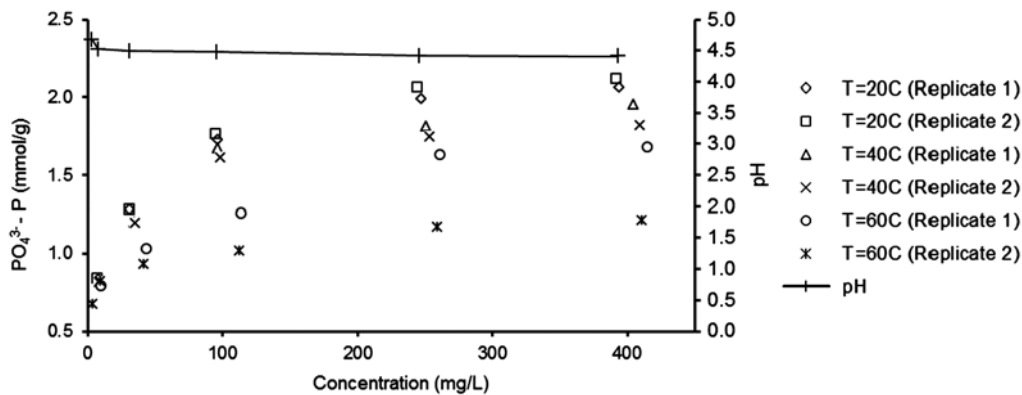
Fig. 7. Adsorption Isotherms for PO_4^{3-}–P sorption onto MPB; contact time: 24 h. Initial pH = 7.
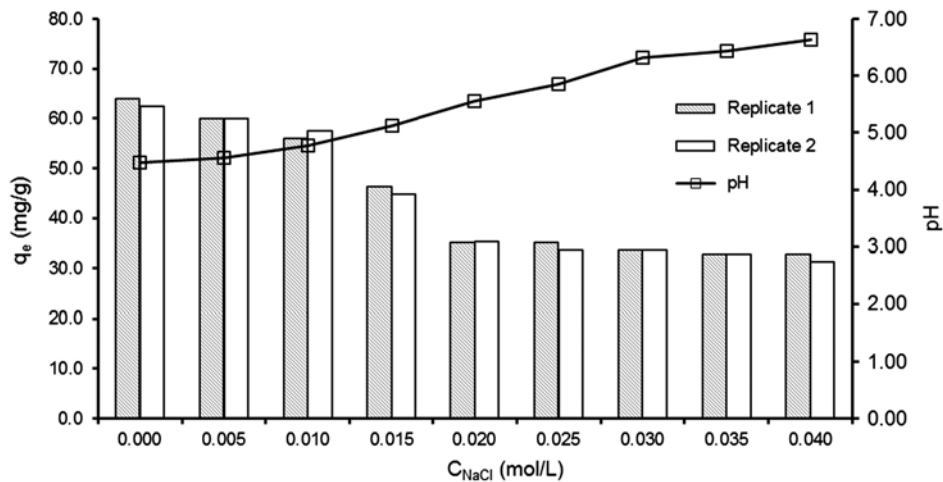
Fig. 8. Effect of ionic strength on the PO_4^{3-}–P uptake by MPB ($C_0 = 200$ mg L^{-1}). Initial pH = 7.

3.10. Removal of PO_4^{3-} from a sludge centrate and the effluent of a dairy farm anaerobic digester

Batch adsorption experiments were conducted to assess the effectiveness of the MPB for PO_4^{3-}–P removal from two field samples. The first sample was the centrate of anaerobically digested sludge solids separated by centrifugation, whereas the second sample was the effluent of a dairy farm anaerobic digester. The initial PO_4^{3-}–P concentration for the two samples was 22.7 mg L^{-1}, 34.0 mg L^{-1}, respectively. The effect

Table 3
Thermodynamic parameters for PO_4^{3-}–P adsorption by MPB

PO_4^{3-}–PC_0 (mg L^{-1})	$\Delta H°$ (kJ/mol)	$\Delta S°$ (J/mol K)	$\Delta G°$ (kJ/mol)		
			$T = 20℃$	$T = 40℃$	$T = 60℃$
100	−6.01	37.93	−17.12	−17.88	−18.64
200	−5.20	32.78	−14.80	−15.46	−16.12
300	−2.79	36.97	−13.62	−14.36	−15.10

of adsorbent dosage on the removal of PO_4^{3-}–P was tested using five different dosages of MPB ranging from 0.5 to 5 g L^{-1}. For the sludge centrate sample, the removal efficiency increased from 19.8% at 0.5 g L^{-1} of MPB dosage to 70.9% at 5 g L^{-1} of MPB dosage. Similarly for the effluent of the dairy farm anaerobic digester the removal efficiency increased from 17.1% at 0.5 g L^{-1} of MPB dosage to 61.5% at 5 g L^{-1} of MPB dosage. Under similar conditions with synthetic PO_4^{3-}–P solutions containing 40 mg L^{-1}, the removal efficiency increased from 24.7% at 0.5 g L^{-1} of MPB dosage to 97.8% at 5 g L^{-1} of MPB dosage. The reduction of the PO_4^{3-}–P removal rate in the field samples compared to the synthetic solution, could be due to competitive ion effect between phosphate and interfering ions.

4. Conclusions

This research demonstrated the efficiency of phosphate removal from water by MPB prepared using green chemistry. The phosphate removal was shown to be concentration and ionic strength dependent, exothermic, spontaneous, and is best described by a pseudo-second-order kinetics. The Zeta potential measurements indicated that PO_4^{3-} removal was due to electrostatic interaction between the grafted quaternary amine groups and the PO_4^{3-} anions. Moreover, the activation energy investigation indicated that the sorption process is governed by ion-exchange. The MPB was successfully regenerated for five sorption cycles without significant loss of PO_4^{3-}—removal efficiency. Finally, the MPB was successfully used to remove PO_4^{3-}—from actual field samples. The PO_4^{3-}-loaded MPB could be potentially used as fertilizer before or after its end of life cycle.

Acknowledgments

References

[1] U.S. Environmental Protection Agency, Office of Water, State Adoption of Numeric Nutrient Standards (1998–2008), US EPA, Washington, DC, 2008.
[2] L.L. Blackall, G.R. Crocetti, A.M. Saunders, P.L. Bond, A review and update of the microbiology of enhanced biological phosphorus removal in wastewater treatment plants, Antonie van Leeuwenhoek 81 (2002) 681–691.
[3] D.A. Burke, Dairy Waste Anaerobic Digestion Handbook, Options for Recovering Beneficial Products from Dairy Manure, Environmental Energy Company, Olympia, WA, 2001.
[4] T. Zhang, K.E. Bowers, J.H. Harrison, S. Chen, Releasing phosphorus from calcium for struvite fertilizer production from anaerobically digested dairy effluent, Water Environ. Res. 82 (1) (2010) 34–42.
[5] P.F. Strom, Technologies to Remove Phosphorus from Wastewater, New Brunswick, NJ, Rutgers University, 2006.
[6] I. Šimkovic, J.A. Laszlo, W. Yue, Q. Yu, Preparation of ion exchangers from bagasse by crosslinking with epichlorohydrin-NH$_4$OH or epichlorohydrin-imidazole, J. Appl. Polym. Sci. 64 (1997) 2561–2566.
[7] U.S. Orlando, A.U. Baes, W. Nishijima, M. Okada, Preparation of agricultural residue anion exchangers and its nitrate maximum adsorption capacity, Chemosphere 48 (2002) 1041–1046.
[8] L.H. Wartelle, W.E. Marshall, Quaternized agricultural by-products as anion exchange resins, J. Environ. Manage. 78 (2006) 157–162.
[9] Q.Y. Yue, W.Y. Wang, B.Y. Gao, X. Xu, J. Zhang, Q. Li, Phosphate removal from aqueous solution by adsorption on modified giant reed, Water Environ. Res. 82 (2010) 374–381.
[10] Y. Wang, B. Gao, W. Yue, Q. Yue, Preparation and utilization of wheat straw anionic sorbent for the removal of nitrate from aqueous solution, J. Environ. Sci. 19 (2007) 1305–1310.
[11] U.S. Orlando, A.U. Baes, W. Nishijima, M. Okada, A new procedure to produce lignocellulosic anion exchangers from agricultural waste materials, Bioresour. Technol. 83 (2002) 195–198.
[12] S. Baidas, B. Gao, X. Meng, Perchlorate removal by quaternary amine modified reed, J. Hazard. Mater. 189 (2011) 54–61.
[13] A. Karachalios, M. Wazne, Nitrate removal from water by quaternized pine bark using choline based ionic liquid analogue, J. Chem. Technol. Biotechnol. 88(4) (2013) 664–671.

[14] D.M. Updegraff, Semi micro determination of cellulose in biological materials, Anal. Biochem. 32 (1969) 420–424.

[15] I.A. Preece, Studies on hemicelluloses. The proximate analysis of box-wood, and the nature of its furfuraldehyde-yielding constituents, Biochem. J. 25 (1931) 1304–1318.

[16] B.L. Browning, Methods of Wood Chemistry, vol. II, Interscience, New York, NY, 1967, pp. 387–414.

[17] A.P. Abbott, T.J. Bell, S. Handa, B. Stoddart, Cationic functionalisation of cellulose using a choline based ionic liquid analogue, Green Chem. 8 (2006) 784–786.

[18] American Public Health Association (APHA), American Water Works Association (AWWA), and Water Environment Federation (WEF), Standard Methods for the Examination of Water and Wastewater, APHA, AWWA, WEF, Washington, DC, 1989.

[19] Y. Li, B. Chen, L. Zhu, Enhanced sorption of polycyclic aromatic hydrocarbons from aqueous solution by modified pine bark, Bioresour. Technol. 101 (2010) 7307–7313.

[20] M.E. Argun, S. Dursun, A new approach to modification of natural adsorbent for heavy metal adsorption, Bioresour. Technol. 99 (2008) 2516–2527.

[21] T.S. Anirudhan, B.F. Noeline, D.M. Manohar, Phosphate removal from wastewaters using a weak anion exchanger prepared from a lignocellulosic residue, Environ. Sci. Technol. 40 (2006) 2740–2745.

[22] W. Cao, Z. Dang, X. Zhou, X. Yi, P. Wu, N. Zhu, G. Lu, Removal of sulphate from aqueous solution using modified rice straw: Preparation, characterization and adsorption performance, Carbohydr. Polym. 85 (2011) 571–577.

[23] K.G. Karthikeyan, M.A. Tshabalala, D. Wang, M. Kalbasi, Solution chemistry effects on orthophosphate adsorption by cationized solid wood residues, Environ. Sci. Technol. 38 (2004) 904–911.

[24] M. Özacar, Phosphate adsorption characteristics of alunite to be used as a cement additive, Cem. Concr. Res. 33 (2003) 1583–1587.

[25] Y.S. Ho, G. McKay, Pseudo-second order model for sorption processes, Process Biochem. 34 (1999) 461–465.

[26] Y.S. Ho, J.C.Y. Ng, G. McKay, Kinetics of pollutant sorption by biosorbents: Review, Sep. Purif. Rev. 29 (2000) 189–232.

[27] A.E. Ofomaja, E.B. Naidoo, S.J. Modise, Kinetic and pseudo-second-order modeling of lead biosorption onto pine cone powder, Ind. Eng. Chem. Res. 49 (2010) 2562–2572.

[28] D. Borah, S. Satokawa, S. Kato, T. Kojima, Sorption of As(V) from aqueous solution using acid modified carbon black, J. Hazard. Mater. 162 (2009) 1269–1277.

[29] P.B. Bhakat, A.K. Gupta, S. Ayoob, S. Kundu, Investigations on arsenic(V) removal by modified calcined bauxite, Colloids Surf. A 281 (2006) 237–245.

[30] W.J. Weber, J.C. Morris, Advances in water pollution research: Removal of biologically resistant pollutants from waste waters by adsorption, Proceedings of International Conference on Water Pollution Symposium, vol. 2, Pergamon Press, Oxford, 1962, pp. 231–266.

[31] W.H. Cheung, Y.S. Szeto, G. McKay, Intraparticle diffusion processes during acid dye adsorption onto Chitosan, Bioresour. Technol. 98 (2007) 2897–2904.

[32] J. Dai, H. Yang, H. Yan, Y. Shangguan, Q. Zheng, R. Cheng, Phosphate adsorption from aqueous solutions by disused adsorbents: Chitosan hydrogel beads after the removal of copper(II), Chem. Eng. J. 166 (2011) 970–977.

[33] X. Xu, B. Gao, Q. Yue, Q. Zhong, X. Zhan, Preparation, characterization of wheat residue based anion exchangers and its utilization for the phosphate removal from aqueous solution, Carbohydr. Polym. 82 (2010) 1212–1218.

[34] I. Langmuir, The adsorption of gases on plane surfaces of glass, mica and platinum, J. Am. Chem. Soc. 40 (1918) 1361–1403.

[35] H. Freundlich, Colloid and Capillary Chemistry, Methuen & Co., London, 1926.

[36] P. Sivakumar, P.N. Palanisamy, Adsorption studies of basic red 29 by a nonconventional activated carbon prepared from *Euphorbia antiquorum* L, Int. J. Chem Tech Res. 1 (2009) 502–510.

[37] P.A. Neale, M. Mastrup, T. Borgmann, A.I. Schäfer, Sorption of micropollutant estrone to a water treatment ion exchange resin, J. Environ. Monit. 12 (2010) 311–317.